Functional analysis of KIT gene structural mutations causing porcine dominant white phenotype by using genome edited mouse models

Guangjie Sun, Xinyu Liang, Ke Qin, Yufeng Qin, Xuan Shi, Peiqing Cong, Deling Mo, Xiaohong Liu, Yaosheng Chen*, and Zuyong He*

State Key Laboratory of Biocontrol, School of Life Sciences, Sun Yat-Sen University, Guangzhou 510006, China

* Correspondence author

E-mail: chyaosh@mail.sysu.edu.cn or zuyonghe@foxmail.com

Abstract

Dominant white phenotype in pigs is considered to be caused by two structural mutations in *KIT* gene, including a 450-kb duplication encompassing the entire *KIT* gene, and a splice mutation (G > A) at the first base in intron 17, which leads to the deletion of exon 17 in mature *KIT* mRNA, and the production of KIT protein lacking a critical catalytic domain of kinase. However, this speculation has not yet been validated by functional studies. Here, by using CRISPR/Cas9 technology, we created two mouse models mimicing the structural mutations of *KIT* gene in dominant white pigs, including the splice mutation mouse model $KIT^{D17/+}$ with exon 17 of one allele of *KIT* gene deleted, and duplication mutation mouse model $KIT^{Dup/+}$ with one allele of *KIT* gene coding sequence (CDS) duplicated. We found that each mutation individually can not cause dominant white phenotype. Splice mutation homozygote is lethal and heterozygous mice present piebald coat. Inconsistent with previous speculation, we found *KIT* gene duplication mutation did not confer the patched phenotype, and had no obvious impact on coat color. Interestingly, combination of these two mutations lead to dominant white phenotype. Further molecular analysis revealed that combination of these two structural mutations could inhibit the kinase activity of the KIT protein, thus reduce the phosphorylation level of PI3K and MAPK pathway associated proteins, which may be related to the observed impaired migration of melanoblasts during embryonic development, and eventually lead to dominant white phenotype. Our study provides a further insight into the underlying genetic mechanisms of porcine dominant white coat colour.

Author summary

KIT plays a critical role in control of coat colour in mammals. Two mutation coexistence in *KIT* are considered to be the cause of the *Dominant white* phenotype in pigs. One mutation is a 450-kb large duplication encompassing the entire *KIT* gene, another mutation is a splice mutation causing the skipping of KIT exon 17. The mechanism of these two mutations of KIT on coat color formation has not yet been validated. In this study, by using genome edited mouse models, we found each structural mutation individual does not lead dominant white phenotype, but combination of these two mutations could lead to a nearly complete white coat colour similar to pig dominant white phenotype, possibly due to the inhibition of the kinase activity of the KIT protein, thus its signalling function on PI3K and MAPK pathways, leading to impaired migration of melanoblasts during embryonic development, and eventually lead to dominant white phenotype. Our study provides a further insight into the underlying genetic mechanisms of porcine dominant white coat colour.

Introduction

Due to domestication and long term selection, dominant white is a widespread coat color among domestic pig breeds, such as Landrace and Large White [1]. The dominant white phenotype in domestic pigs is considered to be caused by two structural mutations in the *KIT* gene, (1) a ~450-kb tandem duplication that encompasses the entire *KIT* gene body and ~150 kb upstream region of KIT gene and (2) a splice mutation at the first nucleotide of intron 17 in one of the *KIT* copies that leads to the skipping of exon 17,

and the production of KIT protein lacking a critical region in kinase catalytic domain. [2-6].

KIT is a class III tyrosine kinase receptor, encoded by the *KIT* gene. KIT receptor is expressed on several cell types, including mast cells, hematopoietic progenitors, melanoblasts and differentiated melanocytes [7]. The binding of its ligand - stem cell factor (SCF) causes KIT to homodimerize, leading to the activation of its intrinsic kinase activity through autophosphorylation of tyrosine residues. KIT has a number of potential tyrosine phosphorylation sites, which interact with multiple downstream signaling pathways, including the PI3K, MAPK, and Src family kinase pathways [7, 8]. These pathways are involved in the regulation of cells growth, survival, migration and differentiation [9].

The 450-kb large duplication that encompasses the entire *KIT* gene body previously was speculated to confer the patch phenotype in pigs due to abnormal KIT expression [4]. Based on this, a hypothesis has been proposed that there is an evolutionary scenario whereby the duplication first occurred and resulted in a white-spotted phenotype that was selected by humans. The splice mutation occurred subsequently and resulted in a completely white phenotype, due to the skipping of exon 17 in the mature transcript removes a crucial part of the tyrosine kinase domain, thus enhances the defect in *KIT* signaling functions [5], and disturbs the migration of melanocyte precursors, leading to dominant white coat colour [2]. This seems

89 reasonable, as normal migration and survival of neural crest-derived melanocyte
90 precursors is dependent on KIT expression and the availability of its ligand [10]. Loss
91 of function mutations in *KIT* gene could lead to white coat color in mouse, as
92 documented in homozygous KIT ^{K641E} mouse [11] and KIT-deficient model W^v/W^v
93 [12]. However, functional analysis of the structural mutations in KIT gene of dominant
94 pigs still need to be carried out to confirm the hypothesis. Here, by using CRISPR/Cas9
95 technology, we created mouse models mimicking the splice mutation and duplication
96 mutation to investigate the underlying genetic mechanism of dominant white
97 phenotype[13].
98

99 # Results

100 **Splice mutation but not the duplication mutation of *KIT* gene leads to altered coat**
101 **color**

102 In pigs, the wild-type KIT allele is recessive and denoted as *i*. Previous studies
103 considered that two different mutant KIT alleles semidominant I^P allele and the
104 dominant *I* allele confer the patch and dominant white phenotype, respectively (Fig.
105 1A). *I* allele presents a 450-kb large duplication (two to three copies) that encompasses
106 the entire *KIT* gene and at least one of the *KIT* copies carries a splice mutation (G>A at
107 the first base in intron 17), causing exon skipping and the expression of a KIT protein
108 lacking an essential part of the tyrosine kinase domain. I^P allele involves the 450-kb
109 duplication but not the splice mutation[6]. To investigate the effects of *KIT* gene
110 structural mutations on coat color, we created three genome edited mouse models using

111 C57BL/6 strain. The C57BL/6 mice is dominant black and broadly used in coat color
112 study [14].
113
114 To mimic the duplication mutation (I^P allele), we knocked in the CDS of KIT gene
115 linked with the enhanced green fluorescent protein (EGFP) reporter via a self-cleaving
116 2A peptide to facilitate subsequent identification (Fig. 1B). The heterologous of *KIT*
117 duplication mouse model was denoted as *KIT* $^{Dup/+}$. Western blot analysis results
118 demonstrated that EGFP was extensively expressed in the skin of *KIT* $^{Dup/+}$ mice, as
119 compared with the wild-type control $KIT^{+/+}$, which implying the inserted *KIT* CDS was
120 correctly expressed, as 2A peptide strategy allows the co-expression of KIT proteins
121 and EGFP from the integrated single vector (Fig. 1D). We found duplication of *KIT*
122 gene did not result in the patch phenotype, as no obvious difference was observed on
123 coat color between *KIT* $^{Dup/+}$ and $KIT^{+/+}$ mice (Fig. 1C).
124
125 To mimic the splice mutation, we substitute the first nucleotide (G) of *KIT* gene
126 intron 17 with A through CRISPR/Cas9 mediated homologous recombination (Fig. 1B).
127 The heterologous of this splice mutation mouse model was denoted as *KIT* $^{GtoA/+}$. An
128 extensive screening of the offspring implies that homologous of splice mutation of KIT
129 gene could be lethal, as no survived individual of *KIT* $^{GtoA/GtoA}$ has been identified. Big
130 white spots appeared on the abdomen of *KIT* $^{GtoA/+}$ mice as compared with $KIT^{+/+}$ (S1
131 Fig). To determine whether the G to A mutation at the first nucleotide of intron 17 of
132 *KIT* gene can lead to the skipping of exon 17, RT-PCR was carried out by using the

133 RNA isolated from the skin of *KIT* $^{GtoA/+}$ mice. To our surprise, the results showed that
134 exon 17 was not removed from the transcript mRNA, and a small percent of the
135 transcript contained partial region of the intron 17, as determined by Sanger sequencing
136 (Fig. 1F & G). As this model does not mimic the splice mutation well, we did not use
137 it in the subsequent studies.
138
139 Therefore, in order to create a mouse model mimicking the skipping of exon 17,
140 we have directly deleted the exon 17 in genomic by using paired sgRNA with one target
141 the intron 16 and another one targets the intron 17 (Fig. 1B). The heterologous of this
142 splice mutation mouse model was denoted as *KIT* $^{D17/+}$. An extensive screening of the
143 offspring implies that homologous of splice mutation of *KIT* gene could be lethal, as no
144 survived individual of *KIT* $^{D17/D17}$ has been identified. In addition, IVF experiment by
145 fertilization oocytes from *KIT* $^{D17/+}$ females with sperm from *KIT* $^{D17/+}$ males resulted
146 in no survived individual of *KIT* $^{D17/D17}$ can be obtained (S1 Table). This confirms the
147 previous speculation that I^{L} allele (single copy of *KIT* gene with the splice mutation)
148 could be lethal in pigs, as this allele was not found among worldwide pig population
149 [6]. RT-PCR analysis of the skin tissue from *KIT* $^{D17/+}$ mice indicates that exon 17 is
150 removed from the mature transcript (Fig. 1E), and this was confirmed by Sanger
151 sequencing (Fig. 1G). Interestingly, compared with *KIT*$^{+/+}$, *KIT* $^{D17/+}$ mice presented a
152 piebald coat colour in head and trunk, a vertical white stripe on the forehead, a half loop
153 of white hair on the shoulder blade area, and dominant white at entire abdominal part.
154 (Fig. 1D & S1 Fig).

Fig 1. Generation of three mouse models mimicking structural mutations of KIT gene in dominant white pig. (A) The schematic summary of *KIT* mutations causing patch and dominant white phenotypes. of three coat phenotypes of pig. The patch coat colour is associated with a 450-kb large duplication that encompasses the entire KIT gene, and the dominant white is a associated with two to three copies KIT gene duplication and at least one of the KIT copies carries a splice mutation (G>A at the first base in intron 17), causing exon skipping and the expression of a KIT protein lacking an essential part of the tyrosine kinase domain. (B) To mimic the duplication mutation of KIT gene in patched pigs, the last exon of KIT gene with stop codon TGA mutated to GCC, linked with the CDS of KIT gene via a self-cleaving 2A peptide, followed by the linking with the enhanced green fluorescent protein (EGFP) reporter via 2A peptide was knocked in to the KIT locus through CRISPR/Cas9 mediated homologous recombination. To mimic the splice mutation, two mouse models were established. One has the first nucleotide (G) of KIT gene intron 17 substitute with A through CRISPR/Cas9 mediated homologous recombination, and another one with the exon 17 deleted by using paired sgRNA with one target the intron 16 and another one targets the intron 17. (C) Coat colour of the wild-type ($KIT^{+/}$), heterologous of KIT duplication ($KIT^{Dup/+}$) and splice mutation ($KIT^{D17/+}$) mouse model. (D) Western blotting analysis confirmed the presence of EGFP expression in the skin of $KIT^{Dup/+}$ mice, implying the inserted *KIT* CDS can be correctly expressed. (E) RT-PCR analysis of the deletion of exon 17 of *KIT* gene in $KIT^{D17/+}$ mice. The truncated PCR product is

177 indicated by arrow head. (F) RT-PCR analysis of the transcription product of *KIT* gene
178 in *KIT* $^{GtoA/+}$ mice. PCR product with insertion is indicated by arrow head. (G) Sanger
179 sequencing of cDNA from F indicates exon 17 of *KIT* gene in *KIT* $^{GtoA/+}$ mice is not
180 removed, and a small percent of the transcript contained partial region of the intron 17.
181 Sanger sequencing of cDNA from E indicates exon 17 is removed from the mature
182 transcript in mature transcript in *KIT* $^{D17/+}$ mice.
183
184 **Splice mutation but not the duplication mutation of *KIT* gene significantly reduces**
185 **melanin accumulation.**
186 Histological analysis (Fontana-Masson staining) of the back skin of 5-week old
187 mice, revealed that similar to the *KIT* $^{+/+}$ control mice, the hair follicles of both *KIT*
188 $^{Dup/+}$and *KIT* $^{D17/+}$ mice are long in length, and in the hair bulb, the dermal papilla is
189 completely coated by matrix, the keratogenous zone region is clearly visible and is
190 connected to hair shaft and dermal papilla, and fibrous tract is substantially invisible in
191 the skin (Fig. 2). These results indicate that similar to the *KIT* $^{+/+}$ control mice, the hair
192 follicles of 5-week-old *KIT* $^{Dup/+}$and *KIT* $^{D17/+}$ mice are in the growing stage (anagen V
193 or VI), which is advantageous for the observation of the hair follicle shape, and melanin
194 distribution due to melanin synthesis is more active during this stage [15]. The results
195 of hair follicle shape imply that both the splice mutation and duplication mutation did
196 not impair the hair follicle development significantly.
197
198 No obvious difference was observed in the content of melanin contained in hair

follicles between *KIT* $^{Dup/+}$ and *KIT* $^{+/+}$ mice (Fig. 2). While almost no melanin is observed in the hair follicles within the white coat area, and the melanin level of hair follicles in the black coat area of *KIT* $^{D17/+}$ is significantly lower (indicated by yellow arrow head). Therefore, the *KIT* duplication mutation did not impair the melanin accumulation, whereas the splice mutation significantly impaired melanin accumulation in hair follicle.

Fig 2. Histological analysis of the back skin of 5-week old *KIT* $^{+/+}$, *KIT* $^{D17/+}$ and *KIT* $^{Dup/+}$ mice. Melanin is stained with Fontana-Masson, and indicated by arrow head. Scale bar = 50 μM.

The piebald coat colour of *KIT* $^{D17/+}$ mice is caused by the reduction of melanocytes.

The reduction of melanin content in hair follicles may be due to reduced melanocytes, or reduced ability of melanocytes on melanin synthesis. To determine the piebald coat of *KIT* $^{D17/+}$ mice is caused by which factor, we used KIT protein as the marker to detect the distribution and amounts of melanocytes in the hair follicle of 5-week-old mice. Compared with the *KIT* $^{+/+}$ control mice, we found that the immunohistochemical staining of KIT decreased in the hair follicles of black coat area of *KIT* $^{D17/+}$mice, while the staining decreased more significantly in the white coat region (Fig. 3A). This was confirmed by qPCR and Western blot analysis of the skin tissues (Fig. 3B and 3C). In theory, the deletion of exon 17 should not affect the expression level of *KIT* gene, thus the reduced *KIT* expression level in skin tissue should

be due to reduced melanocyte quantity. qPCR analysis of the isolated peritoneal cell derived mast cells indicated that deletion of the exon 17 did not affect the expression level of *KIT* gene (Fig. 3B & S2 Fig). The reduced expression of *KIT* gene together with another two marker genes (DCT and Melan A) of melanocytes in *KIT* $^{D17/+}$ mice (Fig. 3C) suggested that the splice mutation of *KIT* gene could lead to reduced number of melanocytes in mice hair follicles.

Unlike the *KIT* $^{D17/+}$mice, the *KIT* $^{Dup/+}$ mice contained an additional copy of *KIT* CDS, which in theory could lead to increased expression of *KIT* gene. qPCR analysis of the isolated mast cells confirmed that the expression level of *KIT* gene was improved in *KIT* $^{Dup/+}$ mice as compared with the *KIT* $^{+/+}$ control mice (Fig. 3B). However, in mouse skin, the expression level of KIT in *KIT* $^{Dup/+}$ mice was not significantly different from the *KIT* $^{+/+}$ control mice as revealed by immunohistochemical and Western blot analysis (Fig. 3A & C). in addition, the expression level of melanocyte marker gene DCT was not affected, but another melanocyte marker gene MelanA was significantly improved in the skin of *KIT* $^{Dup/+}$ mice (Fig. 3C). These results suggested that the duplication mutation of *KIT* gene may not affect the number of melanocytes in the skin, but may affect melanin synthesis.

Interestingly, we observed that the distribution of melanocytes in hair bulb is broader in *KIT* $^{D17/+}$mice as compared with the *KIT* $^{+/+}$ control mice. This phenomenon was more obvious in white coat area than in the black coat area (Fig. 3A). In addition,

243 we found the distribution of melanocytes in the hair bulb of *KIT* $^{Dup/+}$ mice was
244 relatively broader than that in the *KIT* $^{+/+}$ control mice (Fig. 3A). Previous studies
245 considered that only melanocytes that are close to the dermal papilla can secrete and
246 provide melanin to the hair [16], we speculate the altered distribution of melanocyte in
247 both *KIT* splice mutation and duplication mutation mice may have certain impact on
248 melanin accumulation.
249
250 **Fig 3. KIT splice mutation causes the reduction of melanocytes.** (A) Expression of
251 KIT protein in hair follicle of wild-type and mutant mice was determined by
252 immunohistochemical staining. Melanin is stained with Fontana-Masson. Scale bar =
253 50 μM. (B) Transcriptional level of *KIT* gene in mast cell and skin tissue of wild-type
254 and mutant mice was determined by qPCR analysis. (C) Expression level of KIT, DCT,
255 MelanA, AKT, ERK1/2 and phosphorylation level of KIT, AKT, ERK1/2 in skin tissue
256 of wild-type and mutant mice was determined by Western blot analysis. (D)Statistical
257 analysis of relative protein expression levels base on the intensity of bands in C. *
258 stands for $p < 0.05$.
259
260 **Splice mutation of *KIT* gene impairs the kinase activity of the KIT protein and**
261 **affects embryonic melanoblast migration.**
262 Previous studies speculated that *KIT* mutations in dominant white pigs could
263 disturb the migration of melanocyte precursors melanoblasts during the embryonic
264 period [2]. In order to determine whether the splice mutation or the duplication mutation

of *KIT* gene impairs the migration of melanoblasts during embryonic period, we stained the *KIT* protein as a marker to detect the distribution of melanoblasts in the transverse section mice at E14.5. We found no obvious changes in the location of melanoblasts in *KIT* $^{Dup/+}$compared to the *KIT* $^{+/+}$ control mice (S3 Fig). Though the distribution of melanoblasts in *KIT* $^{D17/+}$ near the neural tube is not different between in *KIT* $^{D17/+}$ and the *KIT* $^{+/+}$ mice, the number of melanoblasts in the dorsolateral migration pathway, near the forelimb and the abdomen epidermis is significantly reduced (Fig. 4A). This indicates that duplication mutation of *KIT* gene alone does not impair the migration of melanoblasts, in contrast, the splice mutation could significantly impair the migration of melanoblasts at embryonic stage, however, it does not completely block the migration process, a certain number of melanoblasts could migrate to the corresponding destination positions, and leads to the piebald phenotype.

We observed that, compared with the *KIT* $^{+/+}$ control mice, the colour of black hair of *KIT* $^{D17/+}$ mice became significantly lighter as the mice grew older. The determination of the blackness of mouse hair showed that the blackness of the black hair of *KIT* $^{D17/+}$ mice was comparable to that of *KIT* $^{+/+}$mice at 2 W, however, the blackness of the black hair of *KIT* $^{D17/+}$ mice decreased dramatically at 14 W, and was close to that of white hair of the *KIT* $^{D17/+}$ mice (Fig. 4B). Interestingly, we found the blackness of the hair of *KIT* $^{Dup/+}$mice was relatively lower than that of *KIT* $^{+/+}$mice at 2 W, but became comparable to that of *KIT* $^{+/+}$mice at 14 W (Fig. 4B). Thus, we speculate that the splice mutation of *KIT* gene may affect the renewal or melanin synthesis function of

melanocytes in mice, which in turn causes the blackness of hair to decrease rapidly with age. To examine whether the impaired melanoblast migration and melanocyte renewal is caused by altered kinase activity of the KIT protein receptor, Western blot analysis of the skin tissue was carried out. We found splice mutation significantly reduced the phosphorylation level of KIT protein (Fig. 3C & D), indicating this mutation could lead to impaired autophorylation ability of KIT protein. However, both the expression level and phosphorylation level of AKT, a key protein of the PI3K pathway, was not impaired by the splice mutation of *KIT* gene. Also, the expression of ERK1/2, key proteins of the MAPK pathway, was not affected by the splice mutation, but the phosphorylation level of ERK1/2 was slightly increased (Fig. 3C & D). This result looks confusing, therefore, we further analyzed the expression and phosphorylation levels of AKT and ERK1/2 in follicles by immunohistochemical (IHC) analysis. The amount of target protein was determined by using Combined Positive Score (CPS), which is the number of target protein staining cells divided by the total number of viable cells, multiplied by 100. The results revealed that the expression level of both AKT and ERK1/2 in hair follicles was not affected by the splice mutation of KIT gene (Fig. 4C), however, the phosphorylation levels of these proteins decreased significantly in the follicle of black coat region of *KIT* $^{D17/+}$mice, and phosphorylated AKT and ERK1/2 barely can be detected in the follicle of white coat region of *KIT* $^{D17/+}$mice (Fig. 4C). Western blot results indicate that the duplication mutation of *KIT* gene increased the phosphorylation level of KIT protein (Fig. 3C & D). This is probably due to the increased expression level of KIT protein. Similar to the splice mutation, the duplication mutation did not affect both the

309 expression level and phosphorylation level of AKT. It also did not affect the expression
310 level of ERK1/2, but slightly increased the phosphorylation level of ERK1/2 (Fig. 3C
311 & D). IHC analysis revealed that both the expression level and the phosphorylation
312 levels of AKT and ERK1/2 in the follicle of *KIT*$^{Dup/+}$mice was not significantly affected
313 (Fig. 4C). As AKT and ERK1/2 are respectively involved in the PI3K and MAPK
314 pathways, which are responsible for melanoblast migration and differentiation, and
315 melanin synthesis in melanocyte, therefore, the impaired melanoblast migration and
316 accelerated hair greying in *KIT*$^{D17/+}$mice should be related to impaired function of KIT
317 kinase caused by the splice mutation of *KIT* gene.
318
319 **Fig 4. *KIT* spice mutation affects embryonic melanoblast migration and melanin**
320 **accumulation.** (A) KIT is used as marker to detect melanoblast migration in *KIT* $^{+/+}$
321 and *KIT* $^{D17/+}$ mice embryo (E14.5). Migrating melanoblasts were indicated by arrow
322 heads. Scale bar = 500 μM. (B) Observation of hair from 2-W and 14-W old wild-
323 type and mutant mice under a stereo microscope (left panel). Scale bar = 200 μM. The
324 relative blackness of hair was quantified based on the intensity of image (right panel).
325 * stands for $p < 0.05$. (C) AKT and ERK 1/2 expression and phosphorylation level in
326 hair follicle of wild-type and mutant mice is determined by immunochemical staining.
327 Scale bar = 50 μM.
328

329 **Combination of the splice mutation and duplication mutation of *KIT* gene caused**
330 **severely impaired melanoblast migration during embryonic stage, and dominant**
331 **white phenotype**

332 As the splice mutation and duplication mutation of *KIT* gene individually did not
333 lead to dominant white phenotype, we are curious whether the combination of these
334 two mutations (denoted as compound mutations) can lead to dominant white phenotype.
335 Therefore, the *KIT* $^{Dup/+}$male and the *KIT* $^{D17/+}$female was crossed to produce the *KIT*
336 $^{Dup/D17}$ offspring as determined by PCR analysis of the deleted exon 17 and integrated
337 EGFP reporter (Fig. 5A). Interestingly, the *KIT* $^{Dup/D17}$ mice presented a coat colour
338 resembling the porcine dominant white phenotype: except for few gray hairs appearing
339 near the eyelids and hip, the whole body was covered with white hairs (Fig. 5B). With
340 the increase of age, the gray hairs of the eyelids and hips of *KIT* $^{Dup/D17}$ mice gradually
341 disappeared (S4 Fig). Through histological observation of the back skin of *KIT* $^{Dup/D17}$
342 mice, we found that melanin is hardly visible in the hair follicles (Fig. 5C). However,
343 no apparent morphological difference of the follicle was observed between *KIT* $^{Dup/D17}$
344 mice and the *KIT* $^{+/+}$ control mice. The hair follicles of 5-week-old *KIT* $^{Dup/D17}$mice
345 showed a typical characteristics of the growing stage (anagen V or VI) (Fig. 5C). This
346 indicates that the compound mutation did not affect the development of hair follicle,
347 but severely impaired the accumulation of melanin in hair follicles.
348
349 We suspected that similar to *KIT* $^{D17/+}$mice, the decreased melanin accumulation
350 in the hair follicles of *KIT* $^{Dup/D17}$ mice may be caused by reduced number of

351 melanocytes in the hair follicles. qPCR analysis of the isolated mast cells from *KIT*
352 $^{Dup/D17}$ mice showed that compound mutations lead to improved expression level of *KIT*
353 gene (Fig. 5D), which was mainly due to integrated additional copy of *KIT* CDS. In
354 contrast, the expression level of *KIT* gene decreased significantly in skin tissue of *KIT*
355 $^{Dup/D17}$ mice as determined by qPCR analysis (Fig. 5D), this was further confirmed by
356 Western blot analysis (Fig. 5E). The reduced expression of *KIT* gene together with
357 another three marker genes (DCT, MelanA and S100) of melanocyte in skin tissue of
358 *KIT* $^{Dup/D17}$ mice (Fig. 5E) suggested that compound mutations of *KIT* gene could lead
359 to reduced number of melanocytes in mice hair follicles, which may contribute to the
360 decreased melanin accumulation in the hair follicles of *KIT* $^{Dup/D17}$ mice.
361
362 IHC analysis of the skin tissue confirmed that the number of melanocytes in the
363 hair follicles of *KIT* $^{Dup/D17}$ mice decreased significantly as compared with the *KIT* $^{+/+}$
364 control mice, with only a few layers of melanocytes in close proximity to the dermal
365 papilla visible (Fig. 5C).
366
367 Few gray hairs presented in the whole white background of *KIT* $^{Dup/D17}$ mice at
368 young age, and they disappear gradually as determined by the hair blackness analysis
369 (Fig. 5G & S4 Fig). This implies that the compound mutations of *KIT* gene may affect
370 the renewal of melanocytes in hair follicles.
371
372 To investigate the underlying molecular mechanism of the compound mutations

373 of *KIT* gene on coat colour changing, the kinase function of KIT protein was determined
374 by Western blot analysis of the skin tissue of *KIT* $^{Dup/D17}$ mice. The results showed that
375 the phosphorylation level of KIT in the skin of *KIT* $^{Dup/D17}$ mice is significantly lower
376 than that of the *KIT* $^{+/+}$ control mice (Fig. 5E). Both the expression level and
377 phosphorylation level of AKT, a key protein of the PI3K pathway, decreased
378 significantly. Though the expression of ERK1/2, key proteins of the MAPK pathway,
379 was not affected, but the phosphorylation level of ERK1/2 decreased dramatically (Fig.
380 5E). These results indicate that the compound mutations of *KIT* gene substantially
381 impaired the signaling function of KIT protein receptor on PI3K and MAPK pathways.
382 However, to our surprise, further IHC analysis of the hair follicle showed that
383 phosphorylation of AKT and ERK1/2 in *KIT* $^{Dup/D17}$seems not affected by the compound
384 mutations as determined by CPS (Fig. 5F). This may imply a complex interaction
385 between the splice mutation and duplication mutation of the *KIT* gene.
386
387 The compound mutations of *KIT* gene impaired the signaling function of KIT
388 protein, which in turn could affect melanoblast migration at embryonic stage. Therefore,
389 IHC analysis of the distribution of melanoblasts in the transverse section of *KIT* $^{Dup/D17}$
390 mice at E14.5 by staining the marker protein KIT. The results showed that compared
391 with the *KIT* $^{+/+}$control mice, the number of melanblast in the embryo of *KIT* $^{Dup/D17}$
392 mice increased significantly in the neural tube, and the number of melanoblasts in the
393 dorsolateral migration pathway, the forelimb epidermis and the abdomen epidermis
394 decreased significantly (Fig. 5H). This result indicates that the compound mutations of

395 *KIT* gene severely blocked melanoblast migration at embryonic stage, leading to
396 increased accumulation of melanoblasts in the neural tube of the *KIT* $^{Dup/D17}$ mice, and
397 a coat colour resembling porcine dominant white phenotype.
398
399 **Fig 5. Combination of *KIT* duplication and splice mutation causes severely**
400 **impaired KIT signaling function and melanoblast migration in embryonic stage.**
401 (A) Identification of *KIT* $^{Dup/D17}$ mice through PCR analysis. (B) Coat colour of *KIT*$^{+/+}$
402 and *KIT* $^{Dup/D17}$ mouse. (C) Histological analysis of melanin accumulation in hair
403 follicle of *KIT*$^{+/+}$ and *KIT* $^{Dup/D17}$ mice by Masson Fontana staining, and presence of
404 melanocytes in hair follicle by immuostainging of KIT. Scale bar = 50 μM. (D) KIT
405 mRNA levels mast cell and skin of *KIT*$^{+/+}$ and *KIT* $^{Dup/D17}$ mice were determined by
406 qPCR analysis. (E) Expression levels of KIT, DCT, MelanA, S100, AKT, ERK1/2 and
407 phosphorylation levels of KIT, AKT, ERK1/2 in skin of *KIT*$^{+/+}$ and *KIT* $^{Dup/D17}$ mice
408 skin were determined by Western blot analysis (left panel) and quantified base intensity
409 of bands (right panel). * stands for $p < 0.05$. (F) Expression and phosphorylation level
410 of AKT and ERK 1/2 in hair follicle of *KIT*$^{+/+}$ and *KIT* $^{Dup/D17}$ mice was determined by
411 immunohistochemical analysis. Scale bar = 50 μM. (G) Observation of hair from 2-W
412 and 14-W old of *KIT*$^{+/+}$ and *KIT* $^{Dup/D17}$ mice under a stereo microscope (upper panel).
413 Scale bar = 200 μM. The relative blackness of hair was quantified based on the intensity
414 of image (lower panel). * stands for $p < 0.05$. (H) KIT is used as marker to detect
415 melanoblast migration in *KIT* $^{+/+}$ and *KIT* $^{Dup/D17}$ mice embryo (E14.5). Migrating
416 melanoblasts were indicated by arrow heads. Scale bar = 500 μM.

Discussion

In our study, we created mice models by using CRISPR/Cas9 technology to mimic the structural mutations of *KIT* gene in dominant white pigs. We used *KIT* $^{D17/+}$ mice model to research the effect of coat colour on *KIT* exon 17 deletion and explored the impact mechanism of *KIT* duplication on coat colour by *KIT* $^{Dup/+}$ mice model. We found that the *KIT* duplication did not influence mouse coat colour but *KIT* exon 17 deletion turns black hair of mouse into piebald colour. The experimental results prove that the *KIT* exon 17 deletion reduced the kinase function of KIT and impair it signaling transduction on PI3K and MAPK pathways, which are involved in melanoblast migration, leading to certain percent of melanoblast blocked in migration from dorsal to ventral region during embryo development, resulting in a piebald coat of the mouse. Interestingly, combination of these two mutations lead to dominant white phenotype. In mutation *KIT* $^{Dup/D17}$ mouse embryo, melanoblasts severe blocked in the neural tube that could not migration. Those make *KIT* $^{Dup/D17}$ mouse displaying *domiant white* phenotype (Fig 6).

Fig 6. Schematic summary of the mechanism of KIT structural mutations on coat colour changing. SCF ligand may induce the formation of KIT/KIT ^{D17} dimer in melanoblast of mouse with KIT splice mutation (*KIT* $^{D17/+}$ mouse), and reduced the kinase function of KIT and impair its signaling transduction on PI3K and MAPK pathways, which are involved in melanoblast migration, leading to certain percent of

439 melanoblast blocked in migration from dorsal to ventral region during embryo
440 development, resulting in a piebald coat of the mouse. Improved expression of normal
441 form of KIT protein in mouse with the combination of KIT splice mutation and
442 duplication mutation (*KIT* $^{Dup/D17}$ mouse) may increase the chance of formation of
443 KIT/KIT ^{D17} dimer upon the binding of SCF as compared with that in *KIT* $^{D17/+}$ mice.
444 Given that the amount of SCF ligand is limited, more KIT/KIT ^{D17} dimer presented on
445 the cell surface of melanoblast may significantly reduce it signaling functions, resulting
446 in more severely impaired melanoblast migration, with most melanoblast remaining in
447 the neural tube, and resulting in a completely white coat colour. DM: dermamyotome;
448 NT: neural tube.
449
450 KIT plays key roles in driving the melanocyte migration from the neural crest
451 along the dorsolateral pathway to colonize the final destination in the skin[17].
452 Mutations at the *KIT* gene is associated with the Dominant White coat colour of several
453 important commercial breeds, like Large White and Landrace. The Dominant White
454 coat colour is determined by the duplication of about 450-kb region encompassing the
455 entire KIT gene (copy number variation, CNV) and by the presence of a splice mutation
456 in intron 17 in one of the duplicated copies, that causes the skipping of exon 17[3]. *KIT*
457 allele with two normal *KIT* copies has been considered to cause the presence of
458 pigmented regions (patches) in white pigs[3]. In addition, a hypothesis has been
459 proposed that the *KIT* allele carries a single copy of a mutated *KIT* gene (with splice
460 mutation) that should be lethal if homozygous [3, 18]. These perspectives have not yet

been validated by functional studies in the past decades. Our functional study confirmed that homozygous of the splice mutation in *KIT* gene is lethal, as *KIT* $^{D17/D17}$ mouse could not be obtained. However, whether the lethal is due to anemia in embryonic stage as previously found in *KIT* defect mouse model need to be further validated. We also found that duplication of the *KIT* gene may not contribute to the patch phenotype found in pigs, as both *KIT* $^{Dup/+}$ and *KIT* $^{Dup/Dup}$ mice did not present the patch coat like that on Pietrain pig, but a coat colour basically indistinguishable from the *KIT*$^{+/+}$ control mice (Fig.1C & S1 Fig). Previous study has proposed that increased KIT expression from pig I^{P} may affect ligand availability, which in turn disturbs the migration of melanocyte precursors, resulting in the patch phenotype [2]. This dosage effect may not be true, as our results showed that increased expression level of KIT protein from additional copy of *KIT* gene (*KIT* CDS in our mouse model) seems to have minimal effect on signaling function of KIT protein receptor on PI3K and MAPK pathways (Fig. 3A & 3C), and thus no obvious effect on melanoblast migration, melanocyte and follicle development, and melanin synthesis. In different to KIT duplication presented in I^{P} allele in the pig, in our KIT duplication mouse model, only *KIT* CDS was inserted, the large fragment of regulatory regions was not included. The duplicated copy in I^{P} allele may lack some regulatory elements located more than 150 kb upstream of *KIT* gene body[4], this regulatory mutation may lead to dysregulated expression of one or both copies of KIT, and thus contribute to the patch phenotype. Mutations in other genes responsible for pigmentation in pigs may be associated with the patch phenotype could not be ruled out.

The exon 17 of *KIT* gene encodes the 790-831 amino acids of KIT protein receptor, a highly conserved region of tyrosine kinase domain, which contains Tyr 823 residue that that is conserved in almost all tyrosine kinases, which is phosphorylated during KIT activation and is thought to act to stabilize the stability of KIT tyrosine kinase activity [8]. The splice mutation leading to the lacking of this region is previous considered to be responsible for the impaired KIT signal transduction, and thus the severe defect in the migration and survival of melanocyte precursors. Our IHC analysis of the skin tissue confirmed that the splice mutation can impair KIT signal transduction on PI3K and MAPK pathways (Fig. 4C). PI3K pathway regulates cell growth, proliferation, differentiation and survival [24], and MAPK regulates cell proliferation and apoptosis [25]. In addition, the MAPK pathway is also responsible for phosphorylating and activating MITF, which in turn activates the transcription of mRNAs of several important proteins involved in melanin synthesis, such as Tyrosinase, TRP and TRP2 [19]. The impaired melanoblast migration during embryonic stage (Fig. 4A), and reduced number of melanocyte and melanin accumulation in hair follicle (Fig. 3A) in *KIT* $^{D17/+}$ mice, could be attributed to the impaired PI3K and MAPK signaling induced by the splice mutation.

Previous study proposed an evolutionary scenario whereby *KIT* duplication occurred first and resulted in a white-spotted phenotype, and the splice mutation occurred subsequently and resulted in a completely white phenotype. The presence of

505 one normal *KIT* copy in *I* ensures that white pigs have a sufficient amount of KIT
506 signaling to avoid severe pleiotropic effects on hematopoiesis and germ-cell
507 development [5]. Thus the *KIT* duplication mutation seems to exhibit a rescue function
508 to the splice mutation. Therefore, at first, we expected that the *KIT* duplication could
509 restore the splice mutation in *KIT* $^{Dup/D17}$ mice. However, combination of these two
510 mutations lead to more severely impaired signaling on PI3K and MAPK pathways
511 (Fig.5E & 5F), melanblast migration (Fig. 5H), melanocyte number reduction and
512 melanin accumulation (Fig.5 H), resulting in nearly completely white coat colour (Fig.
513 5B). Thus the *KIT* duplication mutation does not seems to play a rescue role to the
514 splice mutation. The underlying mechanism of the interaction between these two
515 mutations could be very complicated. As the activation of intrinsic kinase activity of
516 KIT receptor dependents on the binding of SCF ligand to form homodimer. Thus we
517 speculated that improved expression of normal form of KIT protein in *KIT* $^{Dup/D17}$ mice
518 may increase the chance of formation of KIT/KIT ^{D17} dimer upon the binding of SCF
519 as compared with that in *KIT* $^{D17/+}$ mice. Given that the amount of SCF ligand is limited,
520 more KIT/KIT ^{D17} dimer presented on the cell surface of melanoblast may significantly
521 reduce the activation of subsequent PI3K and MAPK signaling pathways, resulting in
522 more severely impaired melanoblast migration, and a more pronounced phenotype
523 change in coat colour (Fig. 6).
524
525 Through observation of the light and electron micrograph of a section of skin, a
526 previous concluded that melanocytes and their precursors were absent in the hair bulb

of the dominant white (*I*) pigs, and the dominant white color in the pig is due to a defect in the development of melanocytes [20]. However, we found that the combination of *KIT* duplication mutation and splice mutation did not completely block the melanoblast migration (Fig. 5H), and few melanocytes or their precursors can be detected in the skin hair follicles of *KIT* $^{Dup/D17}$ mice through immunostaining of marker protein of melanocytes (Fig. 5C). This was confirmed by q-PCR and Western blot analysis of additional melanocytes marker proteins in the skin of *KIT* $^{Dup/D17}$ mice (Fig. 5D). In addition, in our unpublished experiments, expression of several melanocyte marker proteins was detected by q-PCR and Western blot in skin tissue of Large White pigs, implying the exist of melanocyte or its precursors in dominant white pigs. These results indicate that the combination of KIT duplication mutation and splice mutation although impair the development of melanocyte severely, but still few melanocyte precursors can migrate to destination.

In coclusion, our study provides a further insight into the underlying genetic mechanisms of porcine dominant white coat colour.

Materials and Methods

Establishment of mouse models

All mouse models are established on the C57BL/6 background by Model Animal Research Center of Nanjing University (China) as described in previous report [21], with minor modifications. Briefly, C57BL/6 mice were kept under a 12/12 h light/dark

549 cycle. To produce zygotes for pronuclear injection, female mice were injected with 5
550 IU pregnant mare's serum gonadotropin (PMSG), and 46–48 h later injected with 5 IU
551 hCG to induce ovulation 10-12 h later. Following the hCG injection, put the females
552 together with male mice in single cages overnight. Fertilized oocytes were isolated from
553 the oviducts for pronuclear injection. To generate *KIT* $^{Dup/+}$ and *KIT* $^{GtoA/+}$mouse model,
554 Cas9 mRNA, sgRNA and the according donor plasmid (Fig. 1B) were injected into the
555 pronuclei of zygotes. To generate *KIT* $^{D17/+}$mouse model, Cas9 mRNA and a pair of
556 sgRNA (Fig. 1B) were injected. All sgRNA sequences are listed in S2 table. Injected
557 zygotes were transferred into the oviducts of surrogate recipient female mice to deliver
558 genome-edited pups. *KIT* $^{Dup/D17}$ mice were obtained by mating *KIT* $^{D17/+}$females with
559 *KIT* $^{Dup/+}$ males because *KIT* $^{D17/+}$males are infertile.
560
561 All procedures were performed in strict accordance with the recommendations of
562 the Guide for the Care and Use of Laboratory Animals of the National Institutes of
563 Health. The protocol was approved by the Institutional Animal Care and Use
564 Committee (IACUC), Sun Yat-sen University (Approval Number: IACUC-DD-16-
565 0901).
566
567 **Mouse genotyping**
568 Mice genotypes are identified by PCR. The tail of 1week old mice are cut off to
569 extract DNA by using a tissue DNA extraction kit (OMEGA). Primers used in PCR are
570 summarized in S2 table.

Mice skin RNAs were prepared using TRIzol (Invitrogen) extraction followed by DNase (Ambion) treatment, and reverse transcription was carried out using the instructions of Reverse Transcription System (Promega).

Primers for mouse genotype identification please refer to S2 table. Polymerase chain reaction (PCR) was carried out using the GeneStar™ PCR Mix system. Each PCR reaction mix contained 1× GeneStar™ PCR Mix buffer, 1.0μM of each primer and about 100 ng DNA template. The procedure in the thermal cycling was an initial 5 min hold at 95 °C, followed by 35 cycles of 30 sec at 95°C, 30 sec at 60°C, and 30 sec at 72°C, and finishing with 10 min incubation at 72°C.

In order to determine the mutant sequences, the PCR products were recovered by OMEGA DNA Gel Recovery Kit, cloned into pMD-18T vector (TAKARA) and transformed into DH5α competent cells. Plasmids then were purified from *E. coli* cells for Sanger sequencing.

Isolation and culture of peritoneal cell derived mast cells

Isolation and culture of peritoneal cell derived mast cells was performed as previous described protocol [22] with minor modifications. 5 ml of PBS and 2 ml of air was injected into peritoneal cavity of 14 weeks old mice. Then injected mice were carefully shaken in the palm for 5 mins. Subsequently, the cell-containing fluid of the

peritoneal cavity is gently collected in a plastic Pasteur pipette. After centrifugation, cells were resuspended, and cultured in DMEM medium supplemented with serum, cytokines IL-3 (CP39; novoprotein) and SCF (C775; novoprotein). After 10 days culture, CD117 and FceR1 makers were used to determine whether cultured cells are mast cell by flow cytometry analysis using the Beckman Coulter Gallios™ Flow Cytometer. For surface staining, cells were stained with APC anti-Mouse CD117 (17-1171; affymetrix) and FITC anti-mouse Fc epsilon receptor I alpha (FceR1) (11-5898; affymetrix) at room temperature for 30 minutes, then washed with PBS and then re-suspended in PBS.

Histological and immunohistochemical analysis of tissue sections

Skin tissues and embryos were fixed overnight in 10% (w/v) paraformaldehyde with 0.02 MPBS (pH 7.2) at 4 °C, processed and mounted in paraffin, then serially cut into 5μm-thick sections by Rotary Microtome (MICROM). Histological sections were stained with hematoxylin and eosin (H&E), observed and photographed under a fluorescent microscopy (Zeiss). For immunohistochemistry experiments, sections were treated with 3% H_2O_2 to quench endogenous peroxidase activity, then treated with 5% bovine serum albumin to block nonspecific protein binding sites. Sections were incubated with primary antibody at 4 ◦C overnight, and then stained by using anti-Rabbit HRP-DAB Cell and tissue staining kit (R&D, CTS005). Detection was followed by TSA plus Fliorescein (Perkinelemer, NEL741001KT). All antibodies including KIT (ab47587; abcam), Phospho-KIT (Try719) (#3391; Cell Signaling), Green Fluorescent

615 Protein (AB3080P; merk), DCT (ab74073; abcam), Erk1/2 (#4695; Cell Signaling),
616 Akt (#9272; Cell Signaling) Phospho-Akt (#4060; Cell Signaling) and Phospho-
617 Erk1/2 (#8544; Cell Signaling) were diluting in 1:200 with PBS.
618
619 **qPCR**
620 For all gene expression level detection, total RNAs were prepared using TRIzol
621 (Invitrogen) extraction followed by DNase (Ambion) treatment, and reverse
622 transcription was carried out following the instructions of Reverse Transcription
623 System (Promega). The resulting total cDNAs were analyzed quantitatively using
624 FastStart Universal SYBR Green Master kit (Roche) with primers for *KIT, ERK, AKT,*
625 *PLCG* and *DCT*. Expression profiles were tested in triplicate on at least two mice on an
626 LC480 instrument (Roche). Data were analyzed using the comparative Ct (ΔΔCt)
627 method and one-tail, unpaired student T test (significance cutoff $p<0.01$). Gene
628 expression levels were normalized to the housekeeping gene glyceraldehyde 3-
629 phosphate dehydrogenase (GAPDH).
630
631 **Western blot analysis**
632 Proteins were extracted using Lysis Buffer (Key GEN), and proteins concentration
633 was determined by using PierceTM BCA Protein Assay Kit (Thermo). 300 ng protein
634 was subjected to 10% SDS gel and electrotransferred onto PVDF membrane (Roche).
635 After blocking for 1h with 3% BSA in PBS, the membrane was incubated with primary
636 antibodies at 4 ◦C overnight.

637

638 The rabbit anti-KIT antibody (ab47587; abcam), rabbit anti-Phospho-KIT (Try719)
639 antibody (#3391; Cell Signaling), rabbit anti-Green Fluorescent Protein antibody
640 (AB3080P; merk), rabbit anti-DCT antibody (ab74073; abcam), rabbit anti-Erk1/2
641 antibody (#4695; Cell Signaling) and rabbit anti-Akt antibody (#9272; Cell Signaling)
642 were diluting in 1:1000, rabbit anti-Phospho-Akt antibody (#4060; Cell Signaling) and
643 rabbit anti-Phospho-Erk1/2 antibody (#8544; Cell Signaling) were diluting in 1:2000,
644 rabbit anti-GAPDH antibody (AP0063; biogot) was diluting in 1:5000 with PBS.
645 Following by 10 min three times washing with TBST, the membrane was then
646 incubated with 1:5000 goat anti-rabbit secondary antibodies (Abcam, ab6721) for 1h at
647 room temperature. Protein bands were visualised using Kodak image station
648 4000MM/Pro (Kodak), according to the manufacturer's instructions, and exposed to
649 FD bio-Dura ECL (FD, FD8020). Protein levels were standardized by comparison with
650 GAPDH.

651

652 **Statistical analysis**

653 All data were analyzed by using EXCEL (version 2016). The data were expressed
654 as the means ± SEM. Only values with $p < 0.05$ were accepted as significance.

655

656 **Acknowledgement:** This work was jointly supported by National Transgenic Major
657 Program (2016ZX08006003-006), National Key R&D Program of China
658 (2018YFD0501200), and Key R&D Program of Guangdong Province

(2018B020203003).

References

1. Wiseman J. A history of the British pig: Duckworth; 1986.

2. Marklund S, Kijas J, Rodriguez-Martinez H, Rönnstrand L, Funa K, Moller M, et al. Molecular basis for the dominant white phenotype in the domestic pig. Genome research. 1998;8(8):826-33.

3. Pielberg G, Olsson C, Syvänen A-C, Andersson L. Unexpectedly high allelic diversity at the KIT locus causing dominant white color in the domestic pig. Genetics. 2002;160(1):305-11.

4. Giuffra E, Törnsten A, Marklund S, Bongcam-Rudloff E, Chardon P, Kijas JM, et al. A large duplication associated with dominant white color in pigs originated by homologous recombination between LINE elements flanking KIT. Mammalian Genome. 2002;13(10):569-77.

5. Andersson L, editor Studying phenotypic evolution in domestic animals: a walk in the footsteps of Charles Darwin. Cold Spring Harbor symposia on quantitative biology; 2010: Cold Spring Harbor Laboratory Press.

6. Rubin C-J, Megens H-J, Barrio AM, Maqbool K, Sayyab S, Schwochow D, et al. Strong signatures of selection in the domestic pig genome. Proceedings of the National Academy of Sciences. 2012;109(48):19529-36.

7. Lennartsson J, Rönnstrand L. Stem cell factor receptor/c-Kit: from basic science to clinical implications. Physiological reviews. 2012;92(4):1619-49.

8. Roskoski R. Structure and regulation of Kit protein-tyrosine kinase—the stem cell factor receptor. Biochemical and biophysical research communications. 2005;338(3):1307-15.

9. Imokawa G. Autocrine and paracrine regulation of melanocytes in human skin and in pigmentary

681 disorders. Pigment cell research. 2004;17(2):96-110.

682 10. Wehrle‐Haller B, Weston JA. Receptor tyrosine kinase‐dependent neural crest migration in

683 response to differentially localized growth factors. BioEssays. 1997;19(4):337-45.

684 11. Rubin BP, Antonescu CR, Scott-Browne JP, Comstock ML, Gu Y, Tanas MR, et al. A knock-in

685 mouse model of gastrointestinal stromal tumor harboring kit K641E. Cancer research. 2005;65(15):6631-

686 9.

687 12. Moniruzzaman M, Sakamaki K, Akazawa Y, Miyano T. Oocyte growth and follicular development

688 in KIT-deficient Fas-knockout mice. Reproduction. 2007;133(1):117-25. doi: 10.1530/REP-06-0161.

689 PubMed PMID: 17244738.

690 13. Bernex F, De Sepulveda P, Kress C, Elbaz C, Delouis C, Panthier J-J. Spatial and temporal patterns

691 of c-kit-expressing cells in WlacZ/+ and WlacZ/WlacZ mouse embryos. Development.

692 1996;122(10):3023-33.

693 14. Slominski A, Paus R, Plonka P, Chakraborty A, Maurer M, Pruski D, et al. Melanogenesis during

694 the anagen-catagen-telogen transformation of the murine hair cycle. Journal of investigative dermatology.

695 1994;102(6):862-9.

696 15. Hou C, Miao Y, Wang X, Chen C, Lin B, Hu Z. Expression of matrix metalloproteinases and tissue

697 inhibitor of matrix metalloproteinases in the hair cycle. Experimental and therapeutic medicine.

698 2016;12(1):231-7.

699 16. Botchkareva NV, Botchkarev VA, Gilchrest BA. Fate of melanocytes during development of the

700 hair follicle pigmentary unit. The journal of investigative dermatology Symposium proceedings.

701 2003;8(1):76-9. doi: 10.1046/j.1523-1747.2003.12176.x. PubMed PMID: 12894999.

702 17. Besmer P, Manova K, Duttlinger R, Huang EJ, Packer A, Gyssler C, et al. The kit-ligand (steel

703 factor) and its receptor c-kit/W: pleiotropic roles in gametogenesis and melanogenesis. Dev Suppl.
704 1993:125-37. PubMed PMID: 7519481.
705 18. Johansson A, Pielberg G, Andersson L, Edfors-Lilja I. Polymorphism at the porcine Dominant
706 white/KIT locus influence coat colour and peripheral blood cell measures. Animal genetics.
707 2005;36(4):288-96. doi: 10.1111/j.1365-2052.2005.01320.x. PubMed PMID: 16026338.
708 19. Lin JY, Fisher DE. Melanocyte biology and skin pigmentation. Nature. 2007;445(7130):843.
709 20. Moller MJ, Chaudhary R, Hellmen E, Höyheim B, Chowdhary B, Andersson L. Pigs with the
710 dominant white coat color phenotype carry a duplication of the KIT gene encoding the mast/stem cell
711 growth factor receptor. Mammalian Genome. 1996;7(11):822-30.
712 21. Tao FF, Yang YF, Wang H, Sun XJ, Luo J, Zhu X, et al. Th1-type epitopes-based cocktail PDDV
713 attenuates hepatic fibrosis in C57BL/6 mice with chronic Schistosoma japonicum infection. Vaccine.
714 2009;27(31):4110-7. doi: 10.1016/j.vaccine.2009.04.073. PubMed PMID: 19410625.
715 22. Meurer SK, Ness M, Weiskirchen S, Kim P, Tag CG, Kauffmann M, et al. Isolation of Mature
716 (Peritoneum-Derived) Mast Cells and Immature (Bone Marrow-Derived) Mast Cell Precursors from
717 Mice. PLoS One. 2016;11(6):e0158104. doi: 10.1371/journal.pone.0158104. PubMed PMID: 27337047;
718 PubMed Central PMCID: PMCPMC4918956.

719

720 Supporting information

721 **S1 Fig. *KIT*$^{GtoA/+}$, *KIT*$^{D17/+}$ and *KIT*$^{Dup/Dup}$ mice phenotype.** (A) White spots appeared
722 on the abdomen of *KIT*$^{GtoA/+}$ *mice as compared with KIT*$^{+/+}$. *KIT*$^{D17/+}$ mice presented
723 a piebald coat colour in head and trunk, a vertical white stripe on the forehead, a half
724 loop of white hair on the shoulder blade area, and dominant white at entire abdominal

region. There was no difference between the coat colour of *KIT*$^{+/+}$ and *KIT*$^{Dup/Dup}$ mice at 14 W old. (B) Schematic diagram of primers designed for identification of *KIT*$^{D17/+}$ and *KIT*$^{Dup/Dup}$ mice identification. (C) PCR identification of the *KIT*$^{D17/+}$ and *KIT*$^{Dup/Dup}$ mice.

S2 Fig. Identification of mouse peritoneal mast cells through flow cytometry analysis. KIT (stained by anti-Mouse CD117 APC) and FcεRI (stained by anti-mouse Fc epsilon receptor I alpha) were used as markers of mast cell.

S3 Fig. Using KIT as marker to detect melanoblast migration in *KIT*$^{+/+}$ and *KIT*$^{Dup/+}$ mice embryo. KIT is used as marker to detect melanoblast migration in *KIT*$^{+/+}$ and *KIT*$^{Dup/+}$ mice embryo (E14.5).

S4 Fig. Coat colour changing of *KIT*$^{Dup/D17}$ mice during growth up. With the increase of age, the gray hairs of the eyelids and hips gradually disappeared.

S1 Table. Homologous of splice mutation of KIT gene could be lethal. Oocytes from superovulated *KIT*$^{D17/+}$ females were *in vitro* fertilized with sperms collected from 5 *KIT*$^{D17/+}$ males, and transferred to 10 surrogate females to generate offspring. No *KIT*$^{D17/D17}$ pups were born but 13 *KIT*$^{+/+}$ and 24 *KIT*$^{D17/+}$ pups were obtained.

S2 Table. Oligos and primers used in this study.

747

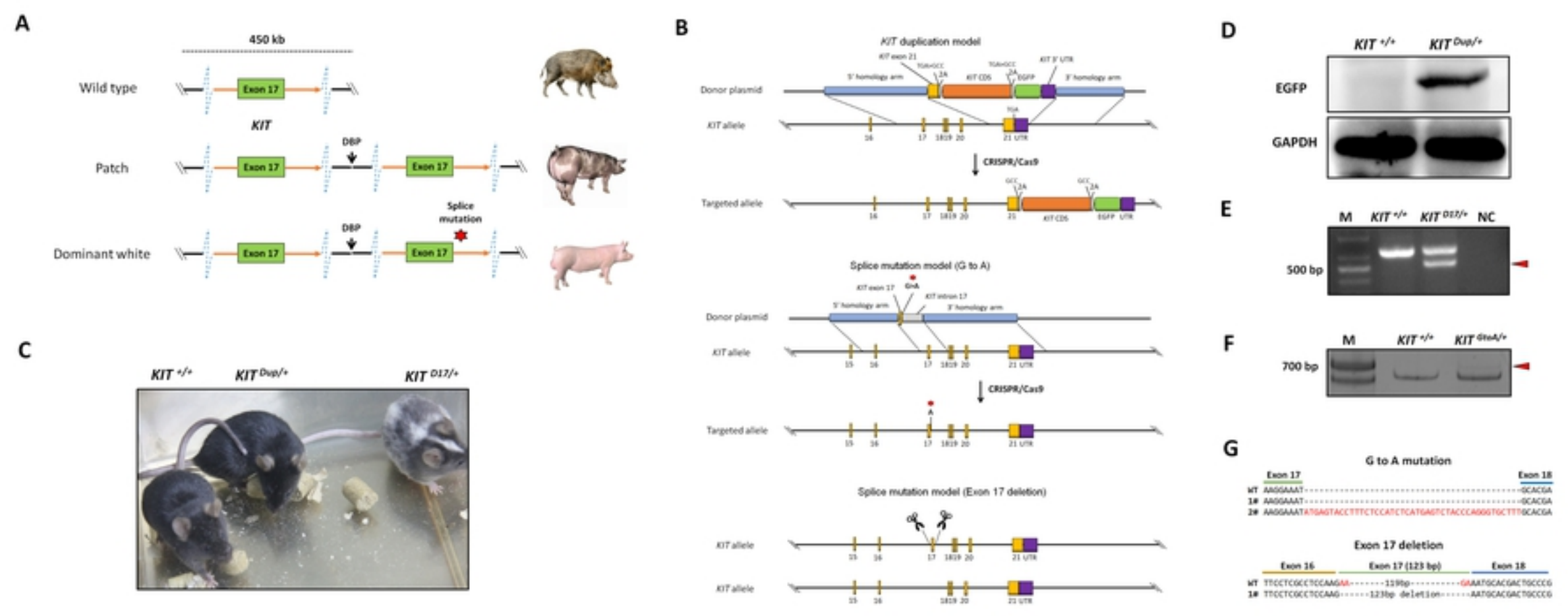
A
450 kb
Wild type
Exon 17
KIT
Patch
DBP
Exon 17
Exon 17
Dominant white
DBP
Splice mutation
Exon 17
Exon 17
B
KIT duplication model
Donor plasmid
KIT allele
CRISPR/Cas9
Targeted allele
Splice mutation model (G to A)
Donor plasmid
KIT allele
CRISPR/Cas9
Targeted allele
Splice mutation model (Exon 17 deletion)
KIT allele
KIT allele
C
KIT +/+
KIT Dup/+
KIT D17/+
D
KIT +/+
KIT Dup/+
EGFP
GAPDH
E
M
KIT +/+
KIT D17/+
NC
500 bp
F
M
KIT +/+
KIT GtoA/+
700 bp
G
G to A mutation
Exon 17
Exon 18
Exon 17 deletion
Exon 16
Exon 17 (123 bp)
Exon 18

Figure 1

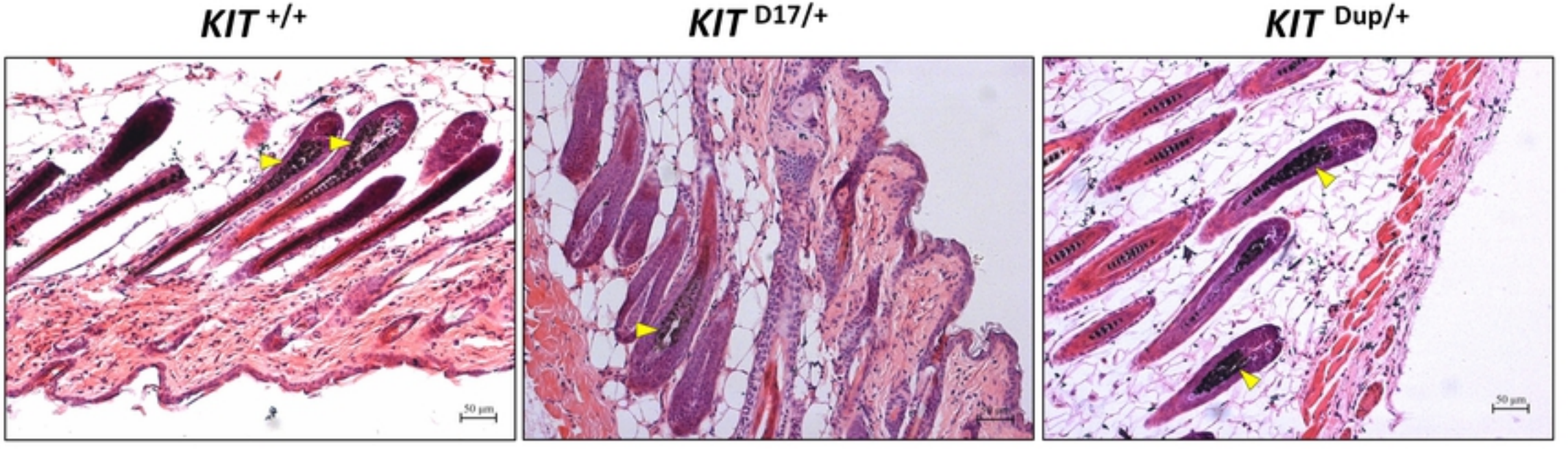

Figure 2

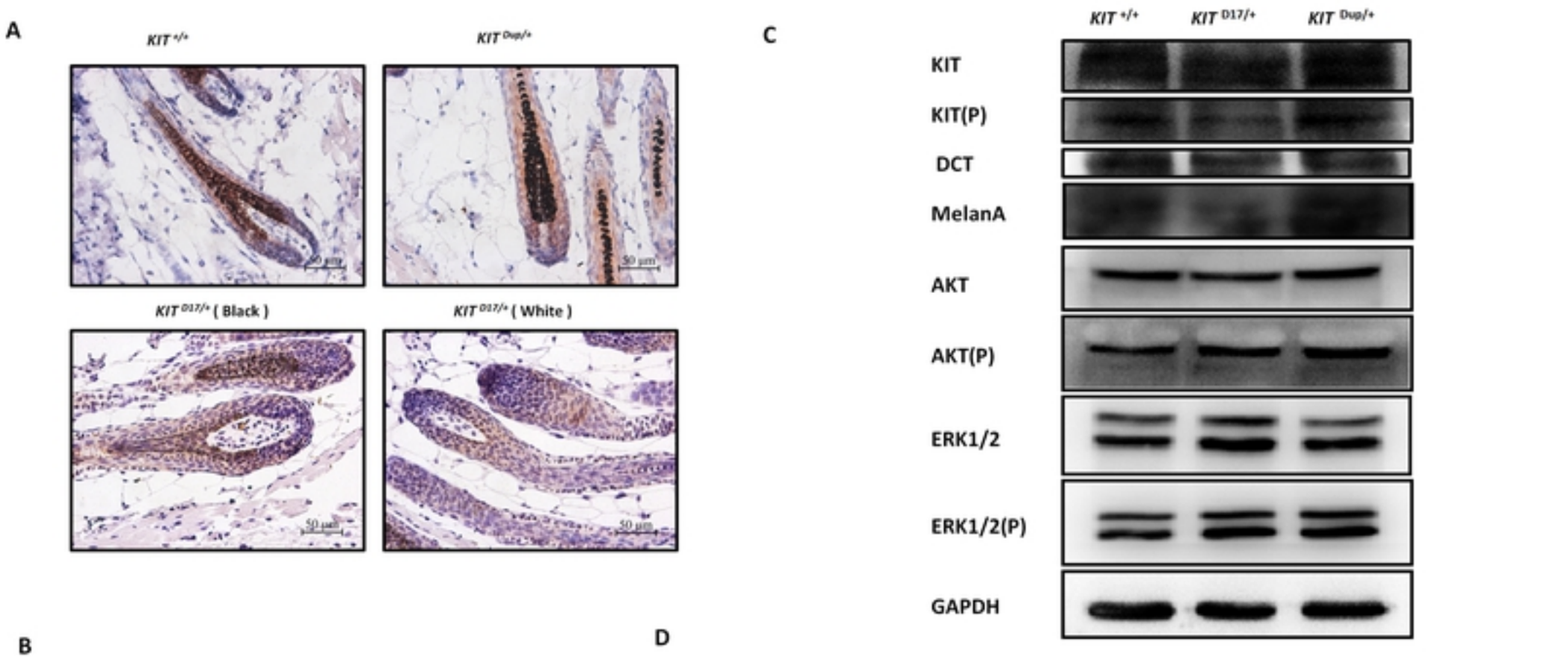
A
KIT +/+
KIT Dup/+
KIT D17/+ (Black)
KIT D17/+ (White)
50 μm
B
Relative mRNA expression levels (KIT/GAPDH)
KIT +/+
KIT D17/+
KIT Dup/+
Mast cell
Skin
C
KIT +/+
KIT D17/+
KIT Dup/+
KIT
KIT(P)
DCT
MelanA
AKT
AKT(P)
ERK1/2
ERK1/2(P)
GAPDH
D
Relative protein expression levels (Protein/GAPDH)
KIT +/+
KIT D17/+
KIT Dup/+
KIT
KIT(p)
DCT
MelanA
AKT
AKT(P)
ERK 1/2
ERK 1/2(P)

Figure 3

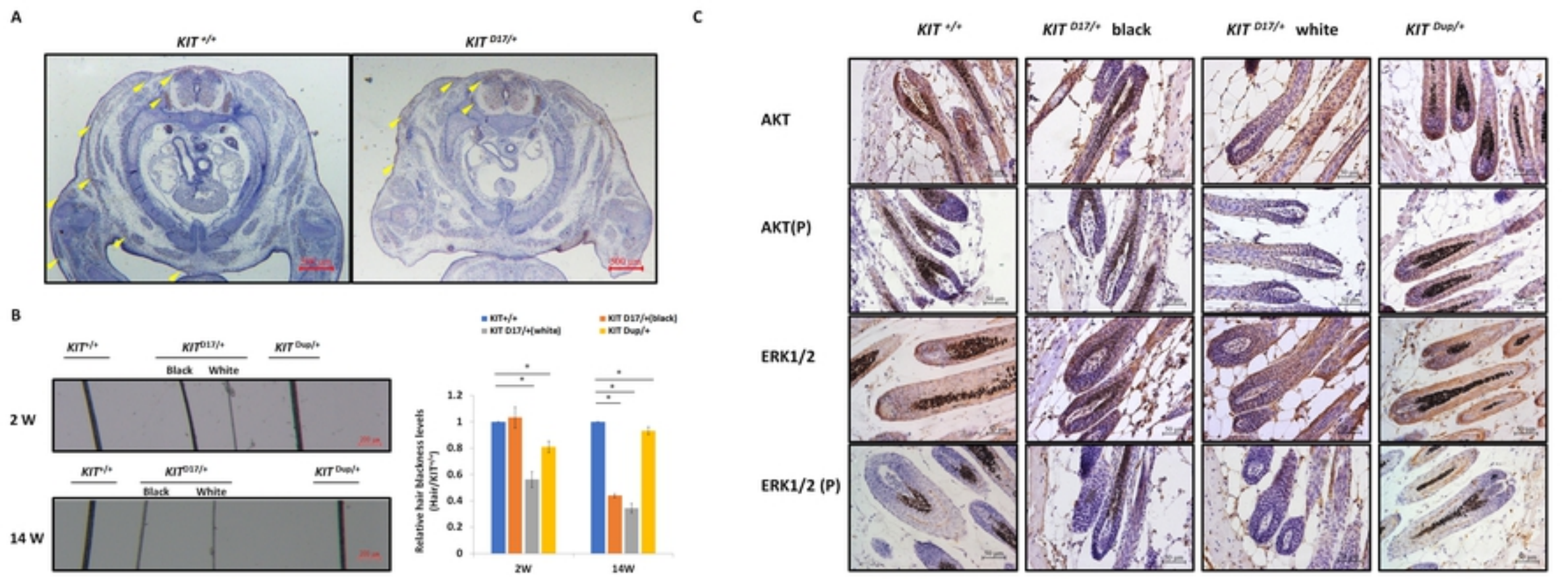
A
KIT +/+
KIT D17/+
B
KIT+/+
KIT D17/+
KIT Dup/+
Black
White
2 W
14 W
KIT+/+
KIT D17/+(black)
KIT D17/+(white)
KIT Dup/+
Relative hair blackness levels (Hair/KIT+/+)
1.2
1
0.8
0.6
0.4
0.2
0
2W
14W
C
KIT +/+
KIT D17/+ black
KIT D17/+ white
KIT Dup/+
AKT
AKT(P)
ERK1/2
ERK1/2 (P)

Figure 4

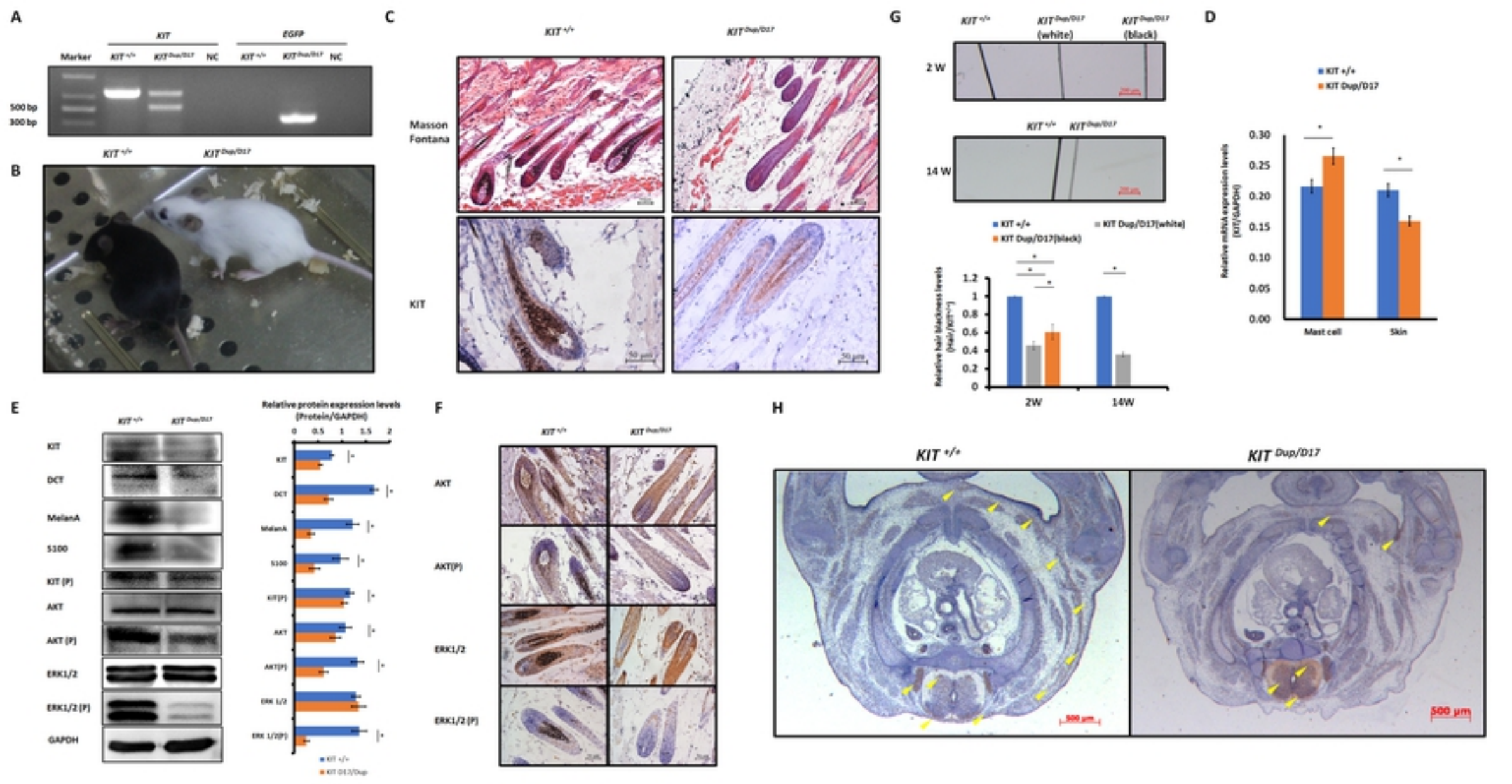
A
KIT
EGFP
Marker
KIT +/+
KIT Dup/D17
NC
500 bp
300 bp
B
KIT +/+
KIT Dup/D17
C
KIT +/+
KIT Dup/D17
Masson Fontana
KIT
50 μm
G
KIT +/+
KIT Dup/D17 (white)
KIT Dup/D17 (black)
2 W
14 W
KIT +/+
KIT Dup/D17(white)
KIT Dup/D17(black)
Relative hair blackness levels (Hair/KIT+/+)
2W
14W
D
KIT +/+
KIT Dup/D17
Relative mRNA expression levels (KIT/GAPDH)
Mast cell
Skin
E
KIT +/+
KIT Dup/D17
KIT
DCT
MelanA
S100
KIT (P)
AKT
AKT (P)
ERK1/2
ERK1/2 (P)
GAPDH
Relative protein expression levels (Protein/GAPDH)
F
KIT +/+
KIT Dup/D17
AKT
AKT(P)
ERK1/2
ERK1/2 (P)
H
KIT +/+
KIT Dup/D17
500 μm

Figure 5

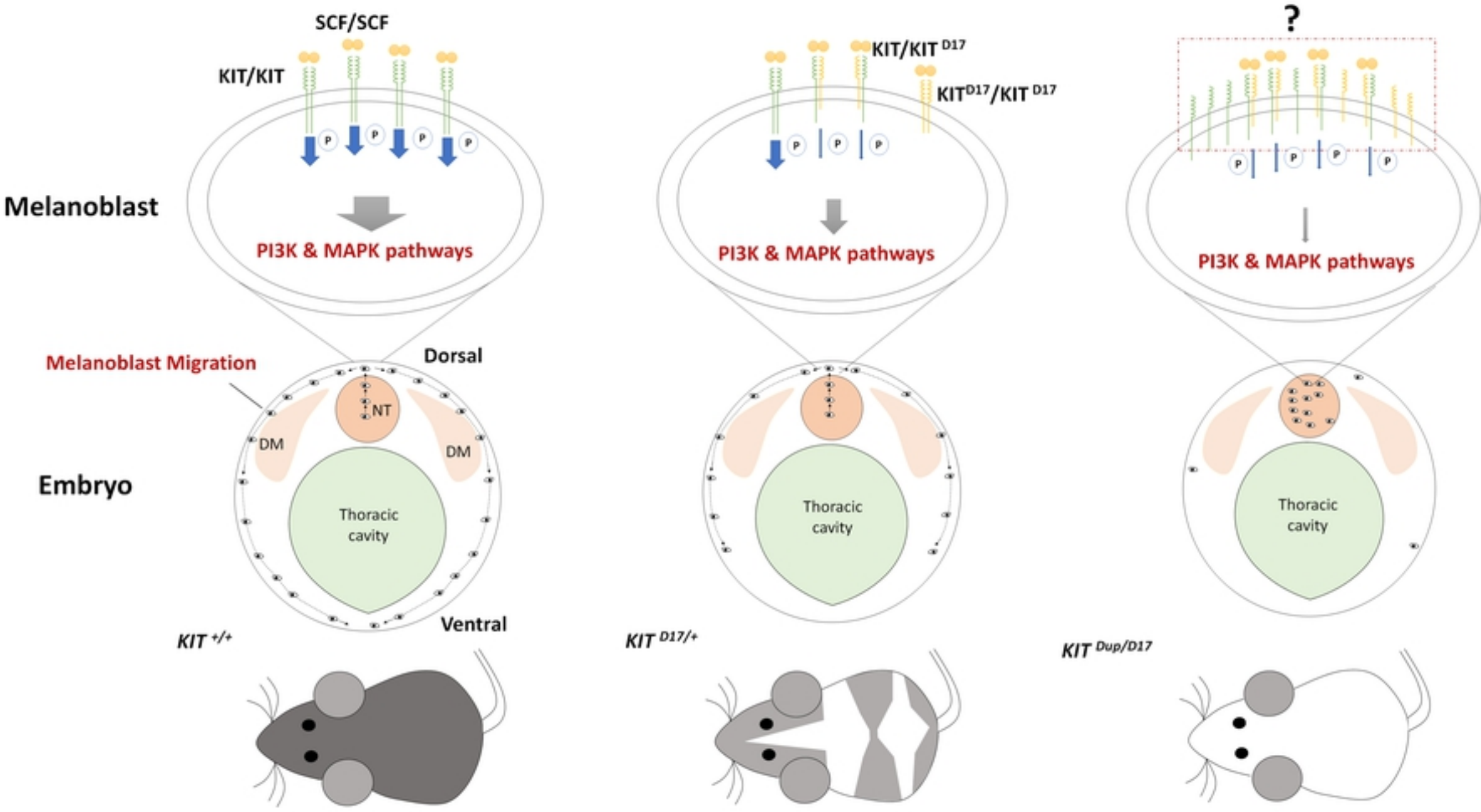
SCF/SCF
KIT/KIT
Melanoblast
PI3K & MAPK pathways
Melanoblast Migration
Dorsal
NT
DM
DM
Embryo
Thoracic cavity
Ventral
KIT +/+
KIT/KIT D17
KITD17/KIT D17
PI3K & MAPK pathways
Thoracic cavity
KIT D17/+
?
PI3K & MAPK pathways
Thoracic cavity
KIT Dup/D17

Figure 6